Impacts of the African Humid Period termination may have been delayed in the Atlantic Sahara

Juliana Nogueira[1,2], Heitor Evangelista[2], Abdelfettah Sifeddine[3], Ahmed ElMouden[4], Lhoussaine Bouchaou[4,5], Yassine Ait Brahim[5], Mercedes Mendez-Millan[3], Sandrine Caquineau[3], Patricia Piacsek[6], Francisco Javier Briceño-Zuluaga[7], Hugues Boucher[3], Carla Carvalho[8], Moussa Masrour[4], Lucie Juřičková[9]

[1] Faculty of Forestry and Wood Sciences, Czech University of Life Sciences Prague. Kamýcká 129. 165 00. Prague, Czech Republic
[2] LARAMG – Radioecology and Climate Change Laboratory, Department of Biophysics and Biometry, Rio de Janeiro State University. Rua São Francisco Xavier, 524. 20550-013. Rio de Janeiro, RJ, Brazil.
[3]IRD, Sorbonne Universite, CNRS, MNHN, IPSL, LOCEAN, Bondy, France.
[4] Laboratory of Applied Geology and Geo-Environment, Ibn Zohr University, Agadir, Morocco.
[5] International Water Research Institute (IWRI), Mohammed VI Polytechnic University (UM6P), Ben Guerir, Morocco.
[6] Centro de Geociencias, Universidad Nacional Autónoma de México (UNAM), Blvd. Juriquilla 3001, Campus UNAM 3001, 76230 Juriquilla, Querétaro, México.
[7] Facultad de Ciencias Básicas - Universidad Militar Nueva Granada, Bogotá, Colombia.
[8] Postgraduate Program in Geosciences (Environmental Geochemistry), Fluminense Federal University, Niterói 24020-141, Brazil.
[9] Department of Zoology, Faculty of Science, Charles University, Viničná 7, CZ-128 44 Praha 2, Czech Republic.

Corresponding author: snogueira.j@gmail.com

ABSTRACT

The paleoenvironmental changes recorded at the Khnifiss Lagoon, on the Saharan Atlantic coast, southern Morocco, during the last 3.5 kyrs BP puts another piece to the puzzle on the intricate relationship between North Atlantic climate patterns and climate variations in Northwest Africa. This study shed light on the hydroclimatic dynamics during a pivotal climatic period: the transition from the mid- to late Holocene and the termination of the African Humid Period. Our research unveils two key periods of salt marsh expansion at the Khnifiss Lagoon, approximately 3.5 and 2.7 kyrs BP when humidity conditions and increased marine influence were recorded. Those conditions paint a scenario of increased storminess and precipitation in NW Africa, compatible with a negative NAO-like climatic configuration. Our data revealed a synchronization between this scenario in NW Africa and cooling events in the North Atlantic during the transition from the mid-to-late Holocene, related to Rapid Climate Changes (RCCs) occurring between 3.5 and 2.5 kyrs BP, also known as the Bond event #2. These findings can potentially enhance climate prediction models, offering opportunities to better prepare for and adapt to the evolving climate patterns in the region. High-resolution paleoenvironmental records are still rare in Northwest Africa and are highly needed. The knowledge gained from these studies represents a critical step towards addressing the climate challenges in Northwest Africa and fortifying the region's resilience in the face of climate change.

Keywords: Africa; Coastal wetlands; Climate change; Holocene; African Humid Period; Paleolimnology; Sedimentology.

INTRODUCTION

Climate change and its impacts on the environment and societies represent one of the most significant challenges of this century. Africa is one of the most climate-vulnerable continents due to the combined effect of its significant exposure to climate change and its low socioeconomic adaptive capacity [1]. In the last decade, the northwest coast of Morocco has been hit by severe winter storms and occasional cyclones, causing extensive damage to the environment and society [2].

Situated along Africa's northern tectonic plates, Morocco faces various meteorological and seismic threats, including earthquakes [3], tsunamis [4], landslides [5], inundations [6], marine storms [2], and the impacts of rising sea levels due to global climate change [7]. Marine winter storms cause intense flooding, beach erosion, and severe damage to roads and tourist facilities [2]. Morocco boasts a coastal zone that stretches for over 3,500 kilometers along the Atlantic Ocean and the Mediterranean Sea, encompassing a maritime area of approximately 1.2 million square kilometers and a fishing potential estimated by the FAO (United Nations Food and Agriculture Organization) at nearly 1.5 million tons, renewable every year [8]. The fishing sector in Morocco is the third most significant contributor to the national economy, following only agriculture and tourism. The Atlantic coast of Morocco is under many human pressures, including urban expansion, pollution, and excessive exploitation of coastal resources [9]. Furthermore, high-energy marine events, such as marine storms, are increasing the stress in the region, leading to short-term inundation of coastal lowlands, posing a threat to people's safety and infrastructure [10].

Therefore, a better understanding of climate change's impact, such as increased storminess, on Moroccan coastal environments and population is needed. However, information on climate change in Northwest Africa, and especially in the Atlantic Sahara, remains scarce, especially from the point of view of long records covering important periods in the Earth's climate history [11].

While the Holocene is generally regarded as a period of relative climatic stability, the transition from the mid to late Holocene was marked by significant environmental changes [12–14]. This shift in Africa represented the transition from the "African Humid Period" during the early Holocene to a drier late Holocene phase [15]. Influenced by enhanced summer insolation over North Africa and the consequent latitudinal displacement and contraction of the Intertropical Convergence Zone (ITCZ), the W Africa monsoonal system underwent a shift in its northward extent [15–19]. The West African monsoonal system was pivotal in governing moisture transport to Northwestern Africa, triggering substantial alterations in the hydrological cycle and vegetation cover [18,20]. Both models [21,22] and proxy-based reconstructions [15,16,23] suggest that this shift led to an amplification of the monsoonal climate system and its northward reach due to feedback mechanisms involving vegetation, soil [24] and extended water bodies [25].

However, several questions surrounding the aridification patterns in Northwest Africa during the mid to late Holocene persist. These inquiries revolve around three key aspects: first, the exact timing of this transition [15,16,26,27]; second, whether this shift towards arid conditions was generally abrupt [18,21,28–30], and finally, the extent of the monsoonal influence reaching northward [28,31,32]. Clarifying these questions is vital for gaining a more comprehensive understanding of the hydroclimatic dynamics during this significant period in the Holocene and the environmental feedback.

North Africa is a pivotal region for examining the intricate connections between low-latitude African monsoon systems and large-scale millennial climate change [33]. The paleoenvironmental reconstruction of coastal deposits provides valuable insights into climate change and sea level changes caused by global to regional-scale exogenic processes [34]. The primary obstacle when it comes to researching Holocene paleoenvironments in arid regions lies in the somewhat limited preservation potential of sediments [35]. This limitation poses a significant challenge to creating a comprehensive climatic change record. For this reason, rare records are found within the region [11,18,36,37] and even fewer are located by the coast [38,39], which underscore the importance of our specific record in the northwestern Sahara region.

In this study, we employ a multiproxy approach to document the paleoenvironmental transformations that have taken place in the Khnifiss Lagoon, located in southern Morocco, over the past 3.5 thousand years Before Present (kyrs BP). By reconstructing the paleoenvironment at this unique site, situated on the Saharan Atlantic coast, we aim to shed light on the hydroclimatic dynamics during a pivotal climatic period: the transition from the mid to late Holocene and the termination of the African Humid Period. Furthermore, the strategic latitudinal position of the Khnifiss Lagoon allows us to assess the interplay of Northern Hemisphere climate patterns and the low-latitude African monsoon system on the hydro-climate of northwest Africa and their variability in the past. Herein, the paleoenvironmental reconstruction of a coastal lagoon in NW Africa recorded the impact of increased storminess over the region and a relative delay in the drying tendency after the mid Holocene, revealing an apparent synchronization between those events and the occurrence of cooling events in the North Atlantic. Given the lack of studies in this important climatic region, we expect that our results will contribute to understanding hydroclimate variability in the transition from mid- to late Holocene and improve climate prediction models that could enhance sustainable development and climate change adaptation.

METHODS

The Khnifiss Lagoon

Situated along the southern Atlantic coast of Morocco, the Khnifiss Lagoon (28°02’54” N, 12°13’66” W) stretches for 20 km in length, covering an expansive surface area of 65 km² (Fig. 1a). The Khnifiss Lagoon, including its salt flats, is the second most important wetland in Morocco and the only tidal lagoon in the desert zone, providing shelter for a highly diverse fauna, including wintering birds [40]. Data from the Ramsar sheet indicate that Khnifiss Park is home to several vulnerable or threatened species at the national or international level.

This coastal lagoon presents a small and shallow basin and rare freshwater input originating from the temporary river (*Oued*) Aouedri. The lagoon is connected to the Atlantic Ocean by a perennial inlet known as *Foum Agoutir*, leaving the lagoon subject to tidal influence [41]. The lagoon features dendritic channels that fill progressively with the tides and narrow upstream. The interconnected tidal channels are flanked by intertidal mudflats, a seagrass bed (*Zoostera*), and an extensive tidal salt marsh, which only floods on the highest tides and boasts a wide variety of vegetation. These salt marshes reveal a clear zoning pattern within the tidal ecosystem, often attributed to the flora’s resilience and adaptation to fluctuating flood and salinity conditions.

The salt marsh extends upstream into the salt flat named *Sebkha Tazra*. However, due to its distance from the inlet, most of *Sebkha Tazra* is unaffected by the tidal cycle and lacks vegetation. During rare periods of rain or exceptionally high spring tides, *Sebkha Tazra* can be briefly flooded [42]. This extensive saltflat depression is enclosed by cliffs, and groundwater lies close to its sandy floor. Due to this configuration, it is possible to observe a thick salt crust formed after the evaporation of groundwater. In the northern and northeast parts of *Sebkha Tazra*, we find transitional areas between salt marsh, desert reg, and salt flat, where small communities of plants grow on small mounds of sand (Fig. 1c).

The Khnifiss Lagoon is under a hot desert climate (BWh), characteristic of dry, arid, low-latitude deserts, according to the Köppen Climate Classification System. Previous works [43–45] describe southwestern Morocco under the influence of interannual to multidecadal timescale climate changes and within the Saharan bioclimatic stage. Wind, humidity, and precipitation in the region are associated with the North Atlantic Oscillation (NAO) phase and the relative position of the Azores anticyclone, as it generates the trade winds that hit the coast obliquely. The very same winds are associated with an important upwelling phenomenon that occurs in the region of the Canary Current (CC), particularly near Cape Ghir, as highlighted by previous research [46] (Fig. 1a). A speleothem from southwestern Morocco revels a millennial long influence of both the NAO and the Atlantic Multidecadal Oscillation (AMO) in the region [44].

Previous research in the Khnifiss Lagoon suggests that, in the last century, the coast was directly affected by NAO oscillations and sea level changes [45]. A combined approach with remote sensing data and geochemical analysis reveals the sensitivity of the Khnifiss Lagoon to large-scale climatic processes, such as NAO. During its positive phase, a strong east-to-west wind leads to a widening of the inlet, which, in turn, affects the hydrodynamics and biogeochemical cycles of the lagoon [45]. Previous studies indicate that the expansion of the Khnifiss Lagoon and surrounding areas is governed by the inlet's dynamic, the sea level of Morocco, and changes in the hydrological condition [45,47]. Therefore, our record has the potential to improve further our knowledge of the climatic mechanisms and dynamics influencing NW Africa environments during the last ~3.5 kyrs BP.

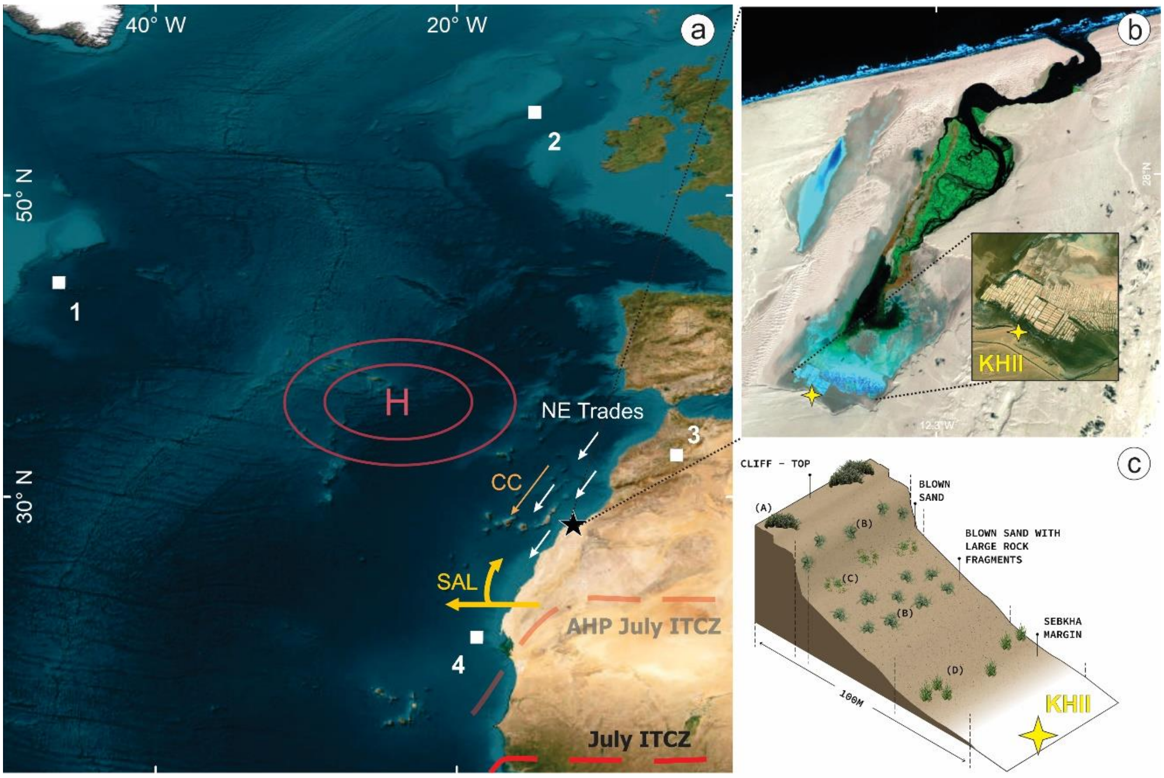

Figure 1 – Geographical, climatic and ecological set of the Khnifiss Lagoon (black star). (a) Climatic mechanisms acting over south Morocco: CC (Canaries Current); SAL (Saharan Air Layer); latitudinal position of the Intertropical Convergence Zone (ITCZ) during winter in the present day (red dashed line) and in the African Humid Period (AHP; faded red dashed line); latitudinal position of the Azores High Pressure Zone (red H); (1) and (2) correspond to the marine cores presented by Bond et al. [48,49] (MC52 + VM29191 and MC21 + GGC22), (3) Pollen reconstruction for the Atlas Mountain based on data from the sediment core at Lake Tigalmamine[50] (4) NW Africa Humidity Index marine sediment core GeoB7920[29]. (b) The Khnifiss Lagoon remote sense image in the composition 543 where the vegetation (green), water (black) and salt flat (*sebkha*; blue) and the position of the KHII sediment core (yellow star) are highlighted. (c) vegetation distribution profile around the coring location.

Sediment core

To deepen our understanding of the region's paleoclimatic dynamics and the changes in its paleoenvironment, we manually collected a sediment core from the innermost area of Sebkha Tazra in the Khnifiss Lagoon (KHII: 27°54 '55.1' N, 12°22'04.4" W) (Fig. 1b).

Before opening, the sediment core was x-rayed using a Siemens 500 ma Polymat S Plus X-ray equipment operating at 85 kVp, 124 mA, 200 mAs. The gray scale of the image was generated using the software ImageJ. The sediment core was opened in half with a subsequent description of the most prominent visible features and the color following the Munsell chart. Subsequently, an X-ray fluorescence (XRF) analysis was performed using an

ARTAX Bruker AXS XRF spectrometer, operating at 25 kV and 500 mA, to obtain the elementary mapping of the sample surface along the sediment core. The sediment core was then sliced into 1-cm subsamples, and visible shells and other mineral specimens were separated for further analysis.

The KHII sediment core was dated at the LMC14 Artemis Laboratory in Saclay, France, according to the following methodology. Samples were treated in an excess of 0.5N hydrochloric acid for several hours at 80°C to eliminate carbonates, then rinsed with ultrapure water until neutral pH. Different quantities, depending on the % Total Organic Carbon (TOC) of the samples, were taken to obtain, after combustion, a volume of CO_2 containing about 1 mg of carbon. The sample was burned in the presence of about 500 mg of copper oxide and a silver wire for 5 hours at 835°C. The CO_2 was then reduced by hydrogen in the presence of iron powder at 600°C. The mass of iron is equal to 3 times the mass of carbon, with a minimum value of 1.5 mg and a maximum value of 4 mg. The carbon deposited on the iron powder and the assembly was pressed into a support for measurement by Accelerator Mass Spectrometry (AMS). The ^{14}C activity of the sample was calculated by comparing the sequentially measured intensities of the ^{14}C, ^{13}C, and ^{12}C beams of each sample with those of CO_2 standards prepared from the reference oxalic acid HOxII and expressed in pMC (percent Modern Carbon) normalized to a deltaC13 of -25 per thousand. Radiocarbon ages were calculated [51] in correcting the fractionation with the deltaC13 calculated from the $^{13}C/^{12}C$ ratio measured on ARTEMIS. The deltaC13 used included fractionation during both sample preparation and the SMA measurement. Measurement uncertainty accounted for both statistical error and measurement variability for the sample and the subtracted blank.

To determine the origin of sedimentary organic matter, elemental and isotopic carbon concentrations were analyzed in samples after acid attack (HCl 3%) to remove the carbonate fraction. $\delta^{13}C$ and organic carbon determination were performed in a FlashHT 2000 elemental analyzer coupled with a Delta V Advantage mass spectrometer from Thermo Fisher Scientific with a precision of 0.05 per mil for $\delta^{13}C$ and 0.05% for organic carbon. The $\delta^{13}C$ is expressed in per mil (‰) against the international standard VPDB (Vienna Pee Dee Belemnite).

For the palynological characterization analysis, thirty-two samples were obtained from the sediment core and prepared. These samples underwent standard laboratory procedures for pollen and spores analysis, as outlined by Faegri and Iversen[52], except for the acetolysis step to preserve the dinocysts. The samples weighed an average of 8-10 g (wet weight) and were sifted through a 150 µm mesh to eliminate larger particles like small stones. Subsequently, the samples underwent decalcification using hydrochloric acid (HCl, 35%) and removal of siliceous content through treatment with cold Fluoclor chemical reagent (40%). Following the chemical treatment, an ultrasonic bath was applied for 30 seconds to disaggregate organic matter. The samples were filtered through a one µm nylon mesh, although particles up to 5 µm might still pass through. These procedures were conducted at the Laboratory of Radioecology and Global Change (LARAMG) within the Department of Biophysics and Biometrics at the State University of Rio de Janeiro, Brazil. The pollen and dinocysts were identified according to the reference collections of Roubik and Moreno[53], and the dinoflagellate cyst types were identified according to Zonneveld and Pospelova[54] morphological descriptions. Both pollen grains and dinoflagellate cysts were counted and presented in relative abundance. We elaborated permanent microscope slides and counted an average of two slides per sample due to the shallow pollen content.

The methodology for particle size analysis followed the established procedure outlined in our previous study [45]. Initially, the samples underwent treatment with 1 N HCl at 25°C to eliminate carbonates. Subsequently, post-digestion, the samples were rinsed with distilled water and subjected to centrifugation at 4000 rpm. The resulting supernatant was meticulously removed using a Pasteur pipette. To eliminate organic matter, concentrated hydrogen peroxide (30%) was added continuously to the samples on a hot plate at 60°C until frothing ceased. A dispersant (sodium hexametaphosphate [NaPO3]6, 40 mg L−1) was introduced to prevent particle aggregation, ensuring an unbiased determination of particle size distribution. The mineral fraction of the sample, devoid of particle agglutination, was obtained after shaking the samples for 24 h. The particle size analysis was conducted using the CILAS® 1064 Particle Analyzer, equipped with a dual sequenced laser system spanning a measuring range of 0.04–500 µm and delivering results in 100 interval classes.

To determine the composition of three mineral specimens recovered from the sediment core, finely crushed sub-samples were deposited on a flat silicon (Si) monocrystal support. X-ray diffraction (XRD) patterns of the samples were recorded on a Panalytical X'Pert Powder diffractometer equipped with a PIXcel detector (255 active channels) and Cu anticathode operating at 40 kV and 40 mA. The diffractograms were measured in the 3°- 70° 2θ range with a step size. Mineral identification was performed using Highscore 3.0 software and two databases: ICSD (Inorganic Crystal Structure Database) and COD (Crystallography Open Database).

Preserved specimens of mollusk shells, preferably whole, were separated for identification during core subsampling. The samples were subjected to an ultrasonic bath for two rounds of one minute using ultrapure water to remove the deposited material. Specimens were identified by specialists at the Department of Zoology, Charles University (Czech Republic) and at the Laboratory of Applied Geology and Geo-Environment, Ibn Zohr University (Morocco), taking into account the species distribution at the Khnifiss Lagoon and later photographed.

A principal component analysis (PCA) was performed using Statistica software by StatSoft to support multi-proxy interpretation and discussion.

RESULTS AND DISCUSSION

The Khnifiss Lagoon paleoenvironment in the last 3.5 kyr

The 207 cm sediment core has shown clear zonation that reflects the paleoenvironmental changes that occurred in the Khnifiss Lagoon (Fig. 2). To understand the timing of those changes, we focused on the portion between 155 and 227 cm of depth and dated four key positioned samples (160-161 cm: 2769 ±27 cal yrs BP,185-186 cm: 6587 ±56 cal yrs BP, 202-203 cm: 3442 ±35 cal yrs BP and 218-219 cm: 3428 ±29 cal yrs BP, Figs. S1 and S2). Dating of coastal lagoons inserted in semi-/arid areas is challenging and outliers, as the one in sample 185-186, can be common [10,55] mainly due to remobilization or periods of intense desiccation cycles. Although, we acknowledge the limitations derived from the reduced number of ^{14}C samples, we are convinced that this chronology should not limit the analysis of the overall trend recorded over the past ~3.5 kyrs and described as it follows.

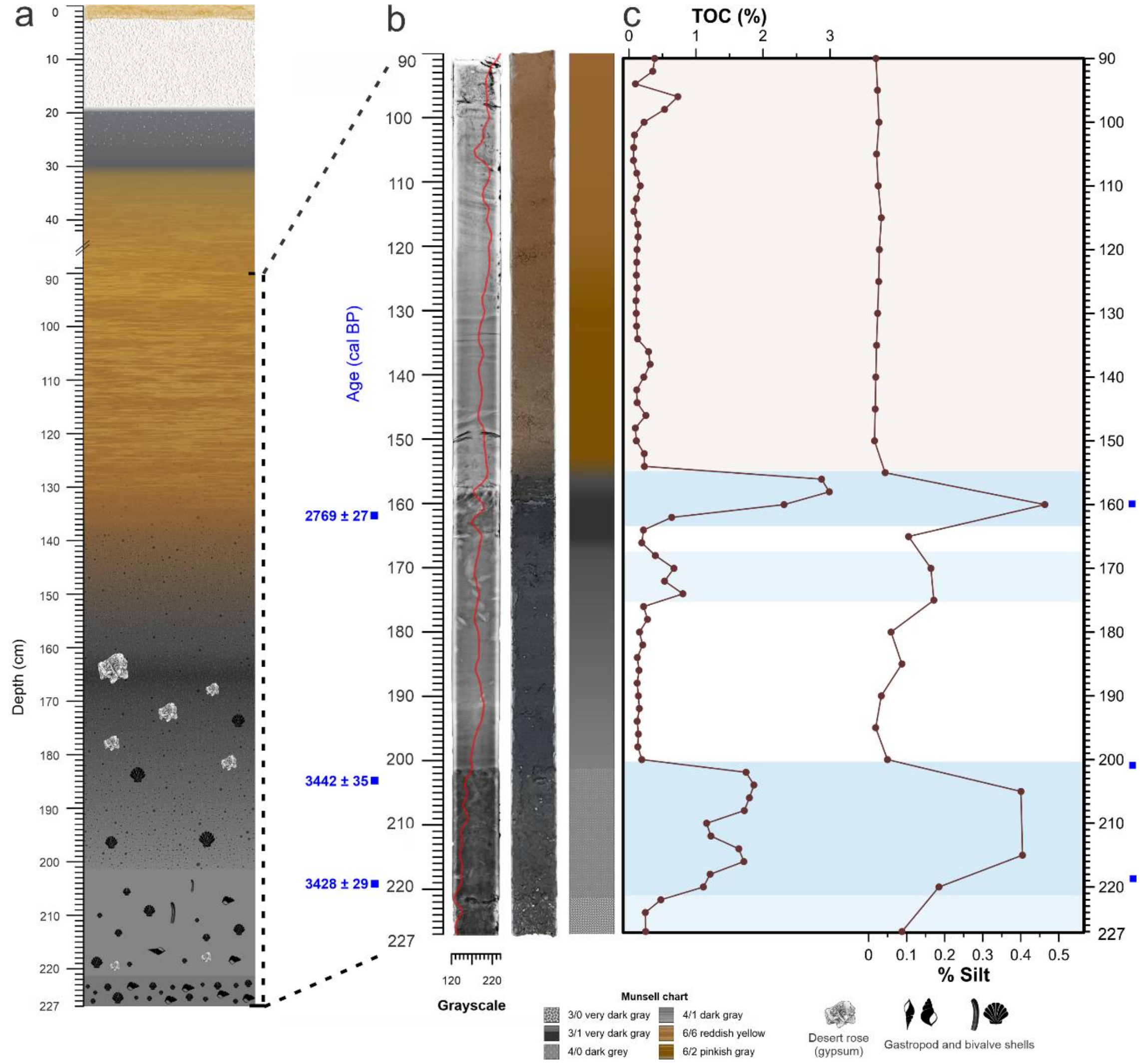

Figure 2 – KHII sediment core profile (a), x-ray (b), photography, and (c) TOC and silt variation. Blue shading represents periods of higher humidity, while orange shading refers to dry periods.

The first phase, corresponding to the period before 3428 ± 29 cal yrs BP (221 – 227 cm), shows a continuous increase of COT (μ = 0.97%), C/N, and silt, followed by a decrease in salinity (Fig. 3), as indicated by the Sr/Ca ratio [45]. In a previous study, the isotope and elemental signatures of vegetation within Khnifiss Park were reported [45]. This information served as the basis for interpreting the C/N vs. $\delta^{13}C$ (Fig. S3), suggesting a combined contribution of submerged vegetation and phytoplankton. The abundant presence of mollusk shells (*Cerastoderma edule*, *Dosinea exoleta*, *Giberulla miliaria*, Calliostomatidae, and Nasaridae; Fig S4) suggests a perennial presence of water during this period. The mentioned species inhabit intertidal muddy sand flats and are also typically associated with Zoostera grass beds. Granulometry during this period indicated a muddy sand substrate characterized by poorly sorted grains that varied in the size of medium sand and very coarse silt. The combined interpretation of the proxies points to an environment with a perennial presence of water and a gradual development of pioneer marsh vegetation [45]. Therefore, a progressive increase in water levels, the related drop in salinity, and the predominance of marine dinoflagellate cysts may indicate a greater marine influence during this period.

The second phase, centered around 3435 ± 32 cal yrs BP (201 – 221 cm), shows an increase in TOC ($\mu = 1.52\%$) content and a displacement towards higher C/N values. The C/N vs. $\delta^{13}C$ diagram points to an increased contribution of eventually submerged salt marsh vegetation. At the same time, the amount of titanium, here used as a proxy for silt/clay minerals [56], increases, reflecting changes in the soil possibly related to marsh development. The prevalence of Chenopodiaceae/Amaranthaceae pollen at notably high percentages indicates an extensive saltmarsh during this phase, as documented by Peglar et al.[57]. It is likely that these pollen grains originated from plants within these taxa, which colonize exposed mud. Concurrently, there was an elevation in the abundance of other pollen types, such as Cyperaceae and Asteraceae. The augmented presence of Cyperaceae is indicative of increased environmental humidity during this period (Fig. S5). During this phase, the dynocists and Amaranthaceae/Chenopodiaceae quantities are invesed, probably due to the increase in the water column in the point of the core retrieval. The large drop in salinity and the continuous presence of marine dinoflagellate cysts and Amaranthaceae/Chenopodiaceae pollen (Fig. 3) corroborate the interpretation of a well-developed salt marsh with high marine influence, as also described for the lagoon Moulay-Boulsalham in north Morocco [58]. Although less abundant, mollusks such as *Cerastoderma edule*, *Odostomia sp.*, *Solen sp.*, *Turitella sp.*, Nassaridae, Mathildidae are still present and are known to typically inhabit Zostera seagrass and intertidal zones, possibly indicating the low tide mark. In general, during phase II there is an established salt marsh, with constant presence of water, increased marine influence, and high sedimentation rate (20 cm deposited around 3435 ± 32 cal yrs BP).

The third and fourth phase, which occurred between 3435 ± 32 cal yrs BP and ~2769 ±27 cal yrs BP (155 – 201 cm), record a dramatic environmental change. At phase III, between 175 and 201 cm, a very low TOC ($\mu = 0.17\%$) is found, and nitrogen values are lower than the detection limit. This could indicate a possible organic matter decomposition, denitrification, and volatilization of nitrogen compounds as the lagoon, at this point, dries out. Furthermore, no dinoflagellate cysts or pollens were found during this period. The grain size analysis shows moderately well and moderately sorted fine and medium sand grains, generally associated with a selective sedimentation agent, such as the wind. Indeed, the x-ray image (Fig. 2b) reveals a lamination pattern of deposition during this phase. Aeolian-deposited sand typically displays wind-ripple laminations characterized by planar-parallel and undulatory layers and fine to medium grains[59]. Thus, a predominant aeolian influence was occurring at the distal point of the Khnifiss Lagoon during the beginning of the third phase. The water would still arrive at this point, probably per percolation initially, and later, towards the end of this phase, forming a shallow water column accompanied by a decrease in salinity. Between 165 and 175 cm, it is possible to observe a significant number of crystalline structures identified by DRX analysis as gypsum rosettes. The presence of these minerals of evaporites is associated with rapid fluctuations of water in an arid environment rich in $CaSO_4$, especially in shallow-water saline lakes and lagoons that go through repeated cycles of dissection [60]. During phase IV, it is possible to observe two brief increases in TOC: the first one centered around 173 cm and the second and highest one centered around 160 cm (i.e., around 2769 ±27 cal yrs BP) that are both accompanied by a drop in salinity. These could indicate a brief return of marine influence, allowing a discreet salt marsh to develop in the distal part of the lagoon. This interpretation is corroborated by the return of the presence of dinocysts andAmaranthaceae/Chenopodiaceae pollen. At the same time, an increase in marine autotrophic organisms is observed, as well as the presence of the pioneer Poaceae (Fig. S5). This phase is abruptly interrupted in 2769 ± 27 cal yrs BP (30 – 155 cm) by dry conditions indicated by a laminated reddish yellow (6/6) sand associated with aeolian transportation and deposition (Fig. 2a,b). No pollen or dynocists are observed in these layers. The well-sorted and rounded sand-grain population shows that the source of aeolian sand may have become dominated by coastal dunes. A thick layer of approximately 16 cm of salt covered by loose sand tops the laminated sand (Figure 2a). The salt crust is then followed by a gray sticky silt layer (4/0 dark gray) of about 10 cm. This layer's average organic carbon content is 0.51%, except for the most recent layer, which presents 2.17%. The presence of crust and grey silt is due to variations in groundwater level, which is linked to variations in local rainfall, sea level, and hydrological changes [61].

We conducted a Principal Components Analysis (PCA) using data on TOC content, Sr/Ca ratio, silt content, and Ti from KHII. Significantly, Figure 3 highlights that the initial principal component contributed substantially by explaining 56% of the variance. It unveils a distinctive pattern characterized by alternating phases of decrease and increase, where the declines are consistently associated with salt marsh accretion. In summary, in contrast to the established *Sebkha* seen today, a developed salt marsh was present ~3435 ± 32 cal yrs BP and ~2769 ±27 cal yrs BP, indicating an advance in the marine influence even in the most continental portions of the lagoon. The current arid condition, therefore, was only completely established after 2769 ±27 cal yrs BP. These significant shifts in environmental parameters highlight the dynamic nature of the region's ecosystem during these particular timeframes.

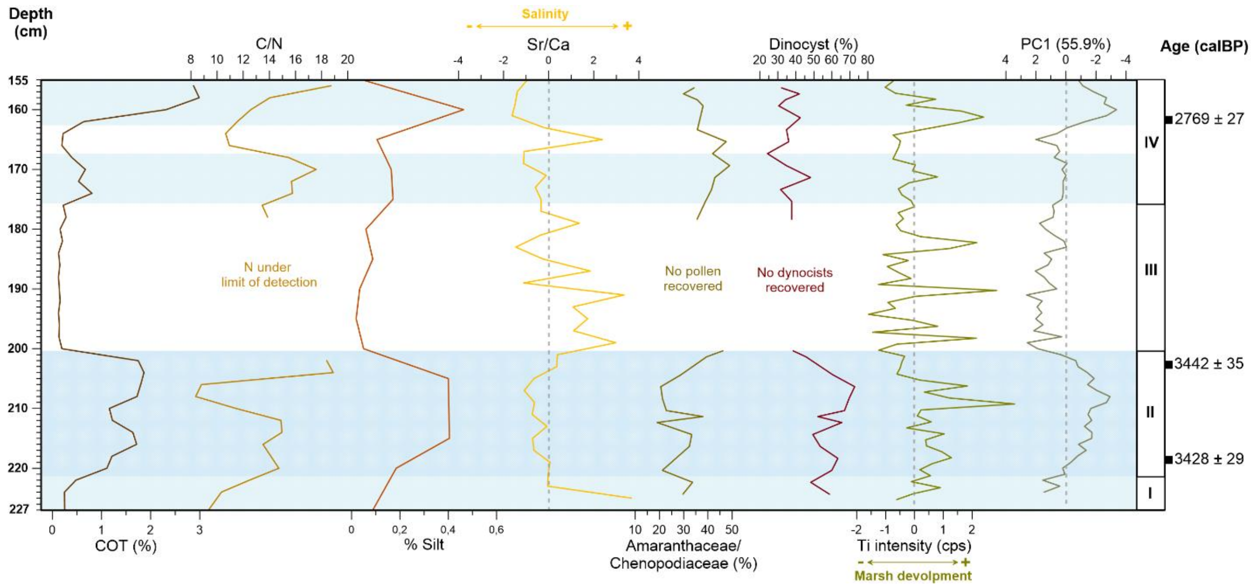

Figure 3 – KHII’s main proxies’ profile and phases I, II and III. Multiproxy analysis of the Khnifiss Lagoon sediment core suggests a developed salt marsh, indicative of increased marine influence in the most continental section of the lagoon, emerged around 3435 ± 32 cal yrs BP and persisted until approximately 2769 ± 27 cal yrs BP, contrasting with the present-day Sebkha. The arid conditions prevailing today were fully established after 2769 ± 27 cal yrs BP.

Holocene Climate Variability and Coastal Responses in Northwest Africa

In the present days, during the boreal winter season, the characteristics of storms, including their location, intensity, and frequency in the North Atlantic, are predominantly influenced by the dynamics of the jet stream and the atmospheric pressure systems within the region. This relationship is elucidated by the NAO index[62], which when during its positive phase, intensified westerly winds push the storm track northward, directing it towards northern Europe. Consequently, this region witnesses warmer and wetter conditions, while northern Africa and southern Europe face drier-than-normal weather. Conversely, during the negative phase, the storm tracks shift southward, resulting in increased precipitation in the western Mediterranean and northern Africa and causing northern Europe to experience colder and drier conditions than usual [63–65].

Throughout the Holocene, both models and paleoclimate reconstructions have indicated that orbital changes led to a progressively steeper temperature gradient and an overall northward shift in the storm track towards the present days [64–68]. In the late Holocene, the northern hemisphere witnessed recurring cooling events, as documented by Bond et al.[69]. These events may have given rise to a scenario reminiscent of a negative phase of the NAO. This climatic pattern, a consequence of the interplay of atmosphere-ocean dynamics, resulted in increased precipitation and storm activity across southern Europe and North Africa [70]. Data from a marine core retrieved off the coast of western Africa (at 20° N) indicates that the Holocene climatic cycles closely paralleled synchronous changes in Sea Surface Temperature (SST), emphasizing a strong in-phase relationship between high- and low-latitude climates [15].

Our sediment core has documented two periods of salt marsh expansion in the most inland portions of the Khnifiss Lagoon in 3.5 kyrs BP (event 1 = E1) and 2.7 kyrs BP (event 2 = E2). Coastal wetlands in arid regions can respond to changes in the i) relative sea level; ii) fluvial apport variation; iii) precipitation amount; iii) wind structure linked to the tidal inlet dynamics; and iv) extreme events such as tsunamis and storms [45,71–74]. At the ebb-dominated Khnifiss Lagoon, previous studies indicated that when storm surges are directed to the continent, increased wave energy causes an enhanced hydraulic slope in the flooding tide within the inlet channel, leading to a net landward movement of sediment and water. This process culminates in the upbuilding of the flood tidal delta – with the deposition of higher grain size – and in the washover of smaller grain size sediments on the salt marsh, allowing its development and expansion [45,47,73,75]. A comprehensive analysis, incorporating both remote sensing data and geochemical assessments, has provided a detailed account of the dynamics within the Khnifiss Lagoon over the past century. This investigation has suggested varying degrees of sensitivity to climatic events depending on the proximity to the lagoon's inlet. Notably, the more inland regions of the lagoon appear to be impacted solely by significant climatic events [45].

To comprehend the dynamics behind progradation events E1 and E2, we have compared the Total Organic Carbon content of the Khnifiss Lagoon sediment core (4a) to other paleoenvironmental studies carried out on the Moroccan Atlantic coast (Fig. 4e) that show high-energy-deposited-sediments occurring at the same time as E1 and E2, suggesting a regional forcing causing these marine transgressions. These on-shore deposits were reported in the form of fine sediments layers at the estuaries of Tahaddart (35.5° N) [10,76] and Loukkos (35.15° N) [4] and at the Moulay-Bousalham (34°N) and Oualidia (32°N) lagoons [38,39,58], and marine gastropods shells deposited at Moulay Douraïne (31° N) [77]. Biogeographic evidence from the NW African coast (28 – 19° N) suggests a transgression event taking place around 3.5 kyrs BP [78], also recorded by wetlands on the Atlantic coast of Spain in addition to another one around 2.8 kyrs BP [79–81]. Changes in Holocene vegetation in France and southwest Spain indicate a humid period between 3.4 and 2.8 kyrs BP, with two arid phases (4.3 – 3.4 kyrs BP and 2.8 – 1.7 kyrs BP) flanking it [82]. Along the Portuguese coast, a humid period occurred around 3 kyrs BP, interrupting the drier conditions that preceded and followed it [83]. Flood frequency records from northeastern Morocco also point to increased precipitation between 3.2 and 2.7 kyrs BP [84]. In the western Mediterranean, increased precipitation recorded around 3.3 and 2.7 kyrs BP [70] coincided with low NAO stages [85]. Both simulations [25] and paleo records [18,28,29,32,55,86–88] indicate humid conditions in the northern Africa around 3 kyrs. On a millennial timescale, coastal areas' sediments can become more or less likely to record overwash deposition according to variations of relative sea level, inlet(s) position and size, and sediment supply changes [10,89,90]. This can lead to variations in the record of events' frequency and intensity in the sediments, resulting in potential delays or omissions when comparing these events across different environments. Nevertheless, the sediment records along the Morocco, Iberian Peninsula, and the Mediterranean point to high-energy events and humid conditions around 3.5 kyrs and 2.8 kyrs BP, impacting as south as 27° N. For the Khnifiss Lagoon, the E2 relative lower sedimentation, when compared to E1, and the abundance of gypsum rosettes during this period are climatically influenced and are a consequence of the rising aridity trend observed in Morocco [91] (Fig. 4f) and NW Africa in general [29] (Fig. 4g) that may have limited the saltmarsh accretion. Peak synchronism among the Khnifiss Lagoon and other proxy records, as evident in Figure 4, indicates an influence of storm surges that probably caused the inlet opening and widening and water to arrive even in the most distant parts of the lagoon. In combination with a more humid climate, the salt marsh thrived in this portion of the lagoon during these events; however, once drier conditions settled in, the marsh gave way to a salt flat, present until these days.

Currently, the climate in our study region is dominated by the baroclinic variation over the North Atlantic [92], and therefore, we hypothesize that our record can be compared to proxies from higher latitudes in the northern hemisphere. Between 3.5 kyrs BP and 2.6 kyrs BP, proxy records point to low temperatures in the Northern Hemisphere, as suggested by the stacked record of Ice-Rafted Debris (IRD) reconstructed in the North Atlantic [14] (namely, Bond #2, Fig. 4b). During the late Holocene, the cooling observed in the North Atlantic region may be attributed to atmospheric-ocean dynamics, including changes in the strength of sub-tropical gyres, as previously explained. This cooling increased precipitation over Northwestern Africa and the Mediterranean, causing a southward shift in the storm tracks. These changes are reflected in the North Atlantic storm index (Fig. 4c; [68]). This climatic scenario is comparable with the present NAO negative phase[93] and is evident in the reconstructed Holocene NAO index[85] (Fig. 4d) and pointed out previously[86]. When reviewing paleoclimate records from diverse global regions, researchers have pinpointed up to six noteworthy periods of rapid climate change (RCC) within the Holocene. A distinct cooling trend in polar regions marked these RCC events. Among these, one particularly significant RCC event unfolded between 3.5 and 2.5 kyrs BP [12,14] that may have been linked with the negative NAO-like scenarios that impacted northwest Africa.

The termination of the African Humid Period (AHP) has been the subject of debate within the scientific community, with most studies convergent on an overall abrupt climatic change occurring at ~5.5 kyrs BP [15,18,94,95]. However, few other studies favor a more gradual transition [21,28,29]. The Khnifiss Lagoon, located at 27°N, currently has a climate dominated by the North Atlantic climate system [92]. However, during the Holocene, this latitude represented the boundary between a dominance by this system at north and a monsoonal climate system dominance at south [18]. In the transition from mid- to late Holocene, this region was under the influence of the northernmost expansion of the West African Summer Monsoon (WASM) [11,28,31,32,36,87]. Therefore, the Khnifiss Lagoon's core, with its sensitivity to the interplay of these two climatic systems, supports the idea of a gradual climate transition in Northwest Africa's coastal regions and records humid conditions until ca 2.7 kyrs BP. This observation agrees with other studies that suggest that a humid period can be clearly recognized from about 5 kyrs BP to 3 kyrs BP in North Africa [96] and until 2 kyrs BP in south Morocco [97]. Hence, we claim that the proposed prolongation of wetter conditions in the Atlantic Sahara was a consequence of the combination of i) RCC events characterized by polar cooling that may have caused an NAO-like scenario that triggered the southward migration and weakening of the Azores High and storminess over north Africa and ii) a northward expansion of the West African Summer Monsoon (WASM). These conditions sustain the concept of a possible teleconnection between hydrological conditions over Northwest Africa and the North Atlantic climatic variability. On a smaller scale, our work, in conjunction with Nogueira et al. [45], highlights the resilience of coastal wetlands to climate fluctuations. It underscores the significant influence of humidity conditions, particularly in arid regions, on salt marsh accretion and inland expansion.

Anticipated global warming may reduce the temperature gradient in mid- to high latitudes, causing winter storm tracks to shift southward and increasing the frequency of storms along Morocco's Atlantic coast[68]. Enhancing our knowledge of the environmental feedback to these changes is crucial in minimizing uncertainties associated with such shifts, which is essential for effective climate adaptation strategies. Furthermore, these climatic alterations may significantly impact the biodiversity of the lagoon, adding an additional layer of ecological complexity. Additionally, given that changes in temperature patterns in the Arctic can influence the biodiversity of the region — home to rare and endemic species — it has the potential to affect local communities dependent on the lagoon for subsistence. Recognizing these interconnected dynamics is vital for a comprehensive understanding of the broader ecological and societal implications stemming from climate-induced shifts.

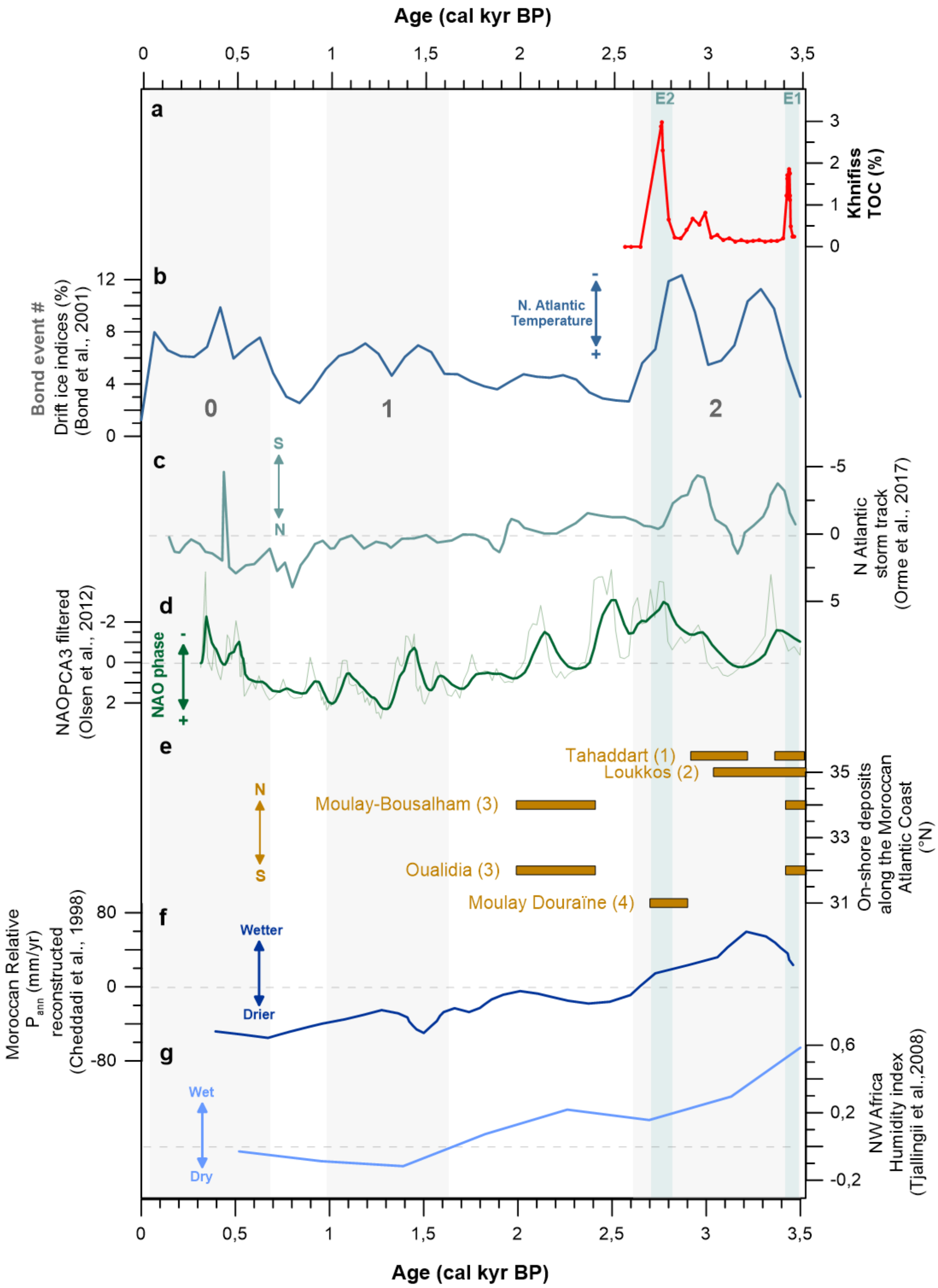

Figure 4 – (a) Khnifiss Total Organic Carbon (TOC) content compared to (b) North Atlantic drift ice indices[48]; (c) North Atlantic storm track reconstruction[98]; (d) North Atlantic Oscillation (NAO) reconstruction[85]; (e) other on-shore deposits along the Moroccan Atlantic coast at: (1) Tahaddart estuary[10], (2) Loukkos estuary[4], (3) Moulay-Boulsalham and Oualidia coastal lagoons[39] and (4) Moulay Douraine[99]; (f) Moroccan relative precipitation reconstruction based on pollen records[50]; and (g) NW Africa Humidity index[29]. Vertical gray bars and numbers represent the different Bond events while green vertical bars mark the timing of high energy progradation events (Event 1: E1, Event 2: E2) recorded at the Khnifiss Lagoon.

CONCLUSION

The challenges posed by climate change in Morocco and Northwest Africa are significant and multifaceted. The region grapples with environmental and societal threats like storms, earthquakes, and rising sea levels, all exacerbated by urbanization and resource exploitation. The research conducted in the Khnifiss Lagoon serves as a valuable window into the transition from the mid to late Holocene, shedding light on the intricate relationship between climate patterns in the North Atlantic and the climate in NW Africa.

The paleoenvironmental reconstruction in the Khnifiss Lagoon has revealed a synchronization between increased storminess and delayed aridification in NW Africa and cooling events in the North Atlantic during the mid- to late Holocene transition. As previously suggested by other researchers, a negative NAO-like scenario could be responsible for such circumstances in south Morocco. At the same time, these conditions must have delayed the aridification trend in the north Saharan coastal environments, which only started after about 2.7 kyrs BP. This suggests that the African Humid Period termination, usually regarded as ca 5.5 kyrs BP, must have happened at different times across North Africa due to environmental specificities. More research on the exact time and nature of these changes, extending the knowledge further back in the past with high resolution archives is needed to understand the extension of the impacts and the climatic feedback between NW Africa and conditions in the North Atlantic.

The emphasis on understanding the dynamic interplay between climate fluctuations and coastal environments highlights the resilience and adaptability of these regions. With the specter of global warming on the horizon, research focusing on predicting possible changes in storm patterns along Morocco's Atlantic coast is necessary. These findings can potentially enhance climate prediction models, offering opportunities to better prepare for and adapt to the evolving climate patterns in the region. Overall, the knowledge gained from these studies represents a critical step towards addressing the climate challenges in Northwest Africa and fortifying the region's resilience in the face of climate change.

REFERENCES

1. Niang, I. *et al.* Africa. in *Climate Change 2014: Impacts, Adaptation and Vulnerability - Contributions of the Working Group II to the Fifth Assessment Report of the Intergovernmental Panel on Climate Change.* 1199–1265 (Cambridge University Press, 2014).
2. Mhammdi, N. *et al.* Marine storms along the Moroccan Atlantic coast: An underrated natural hazard? *Journal of African Earth Sciences* **163**, 103730 (2020).
3. Cherkaoui, T. & El Hassani, A. Seismicity and Seismic Hazard in Morocco 1901-2010. *Bulletin de l'Institut Scientific* **34**, 45–55 (2012).
4. Mhammdi, N. *et al.* Sedimentary evidence of palaeo-tsunami deposits along the Loukkos estuary (Moroccan Atlantic Coast). *Jounal of Tsunami Society International* **34**, 83–100 (2015).
5. Harmouzi, H. *et al.* Landslide susceptibility mapping of the Mediterranean coastal zone of Morocco between Oued Laou and El Jebha using artificial neural networks (ANN). *Arabian Journal of Geosciences* **12**, 696 (2019).
6. *Wadi Flash Floods*. (Springer Singapore, 2022). doi:10.1007/978-981-16-2904-4.
7. Satta, A., Snoussi, M., Puddu, M., Flayou, L. & Hout, R. An index-based method to assess risks of climate-related hazards in coastal zones: The case of Tetouan. *Estuar Coast Shelf Sci* **175**, 93–105 (2016).
8. Royaume du Maroc. *Portrait de secteur de pêche maritime au Maroc*. (2015).
9. Snoussi, M., Khouakhi, A. & Niang-diop, I. Geomorphology Impacts of sea-level rise on the Moroccan coastal zone : Quantifying coastal erosion and fl ooding in the Tangier Bay. **107**, 32–40 (2009).
10. Khalfaoui, O., Dezileau, L., Degeai, J. P. & Snoussi, M. A late Holocene record of marine high-energy events along the Atlantic coast of Morocco: new evidences from the Tahaddart estuary. *Geoenvironmental Disasters* **7**, (2020).
11. Ait Brahim, Y., Bouchaou, L. & Wanaim, A. Speleothem-based paleoclimate research in South Morocco: Interest and perspectives. *Frontiers in Science and Engineering* **11**, 9–16 (2021).
12. Mayewski, P. a. *et al.* Holocene climate variability. *Quat Res* **62**, 243–255 (2004).
13. Haug, G. H. Southward Migration of the Intertropical Convergence Zone Through the Holocene. *Science (1979)* **293**, 1304–1308 (2001).
14. Bond, G. *et al.* Persistent solar influence on north atlantic climate during the Holocene. *Science (1979)* **294**, 2130–2136 (2001).
15. deMenocal, P. *et al.* Abrupt onset and termination of the African Humid Period: *Quat Sci Rev* **19**, 347–361 (2000).
16. Claussen, M., Kubatzki, C., Brovkin, V. & Ganopolski, A. Simulation of an abrupt change in Saharan vegetation in the mid-Holocene. *Geophys Res Lett* **26**, 2037–2040 (1999).
17. Haug, G. H., Hughen, K. A., Sigman, D. M., Peterson, L. C. & Röhl, U. Southward migration of the intertropical convergence zone through the holocene. *Science (1979)* **293**, 1304–1308 (2001).
18. Kuhlmann, H., Meggers, H., Freudenthal, T. & Wefer, G. The transition of the monsoonal and the N Atlantic climate system off NW Africa during the Holocene. *Geophys Res Lett* **31**, 1–4 (2004).

19. McGee, D., Donohoe, A., Marshall, J. & Ferreira, D. Changes in ITCZ location and cross-equatorial heat transport at the Last Glacial Maximum, Heinrich Stadial 1, and the mid-Holocene. *Earth Planet Sci Lett* **390**, 69–79 (2014).

20. Kuhlmann, H., Freudenthal, T., Helmke, P. & Meggers, H. Reconstruction of paleoceanography off NW Africa during the last 40,000 years: Influence of local and regional factors on sediment accumulation. *Mar Geol* **207**, 209–224 (2004).

21. Tierney, J. E., Pausata, F. S. R. & DeMenocal, P. B. Rainfall regimes of the Green Sahara. *Sci Adv* **3**, (2017).

22. Jolly, D., Harrison, S. P., Damnati, B. & Bonnefille, R. Simulated climate and biomes of Africa during the late Quaternary: Comparison with pollen and lake status data. *Quat Sci Rev* **17**, 629–657 (1998).

23. Shanahan, T. M. *et al.* Atlantic forcing of persistent drought in West Africa. *Science (1979)* **324**, 377–380 (2009).

24. Claussen, M., Dallmeyer, A. & Bader, J. *Theory and Modeling of the African Humid Period and the Green Sahara*. vol. 1 (Oxford University Press, 2017).

25. Specht, N. F., Claussen, M. & Kleinen, T. Simulated range of mid-Holocene precipitation changes from extended lakes and wetlands over North Africa. *Climate of the Past* **18**, 1035–1046 (2022).

26. Kröpelin, S. *et al.* Climate-Driven Ecosystem Succession in the Sahara: The Past 6000 Years. *Science (1979)* **320**, 765–768 (2008).

27. Bloszies, C., Forman, S. L. & Wright, D. K. Water level history for Lake Turkana, Kenya in the past 15,000years and a variable transition from the African Humid Period to Holocene aridity. *Glob Planet Change* **132**, 64–76 (2015).

28. Höpker, S. N. *et al.* Pronounced Northwest African Monsoon Discharge During the Mid- to Late Holocene. *Front Earth Sci (Lausanne)* **7**, 1–17 (2019).

29. Tjallingii, R. *et al.* Coherent high- and low-latitude control of the northwest African hydrological balance. *Nat Geosci* **1**, 670–675 (2008).

30. Armitage, S. J., Bristow, C. S. & Drake, N. A. West African monsoon dynamics inferred from abrupt fluctuations of Lake Mega-Chad. *Proceedings of the National Academy of Sciences* **112**, 8543–8548 (2015).

31. Faure, H. Changements climatiques au sud des regions mediterranennes: le Sahara et le Sahel au Quaternaire. in *Quaternary climate in Western Medi- terranean* (ed. Lopez-Vera, F.) 533–534 (Universidad Autonoma, 1986).

32. Wengler, L. & Vernet, J. L. Vegetation, sedimentary deposits and climates during the Late Pleistocene and Holocene in eastern Morocco. *Palaeogeogr Palaeoclimatol Palaeoecol* **94**, 141–167 (1992).

33. Weldeab, S., Lea, D. W., Schneider, R. R. & Andersen, N. 155,000 Years of West African Monsoon and Ocean Thermal Evolution. *Science (1979)* **316**, 1303–1307 (2007).

34. Ghandour, I. M. *et al.* Mid-Late Holocene Paleoenvironmental and Sea Level Reconstruction on the Al Lith Red Sea Coast, Saudi Arabia. *Front Mar Sci* **8**, 1–20 (2021).

35. Ritchie, J. C., Eyles, C. H. & Haynes, C. V. Sediment and pollen evidence for an early to mid-Holocene humid period in the eastern Sahara. *Nature* **314**, 352–355 (1985).

36. Sha, L., Brahim, Y. A., Wassenburg, J. A., Yin, J. & Peros, M. How Far North Did the African Monsoon Fringe Expand During the African Humid Period ? Insights From Southwest Moroccan Speleothems Geophysical Research Letters. 93–102 (2019) doi:10.1029/2019GL084879.

37. Baqloul, A. *et al.* Climate and land-use effects on hydrological and vegetation signals during the last three millennia: Evidence from sedimentary leaf waxes in southwestern Morocco. *Holocene* **31**, 699–708 (2021).

38. Raynal, J. & Ballouche, A. Nouvelles données sur la formation des systèmes lagunaires atlantiques marocains pendant le cycle mellahien. (1985) doi:10.13140/RG.2.1.2517.3928.

39. Ballouche, A. & Carruesco, C. Evolution holocène d'un écosystème lagunaire : la lagune de Oualidia (Maroc atlantique). *Revue de géologie dynamique et de géographie physique* **27**, 113–118 (1986).

40. Beaubrun, P.-C., Thevenot, M. & Schouten, J. R. Wintering and summering water bird populations in the Khnifiss Lagoon. in *The Khinifiss lagoon and its sorrouding environment (Province of L'ayoune, Morocco)* (eds. Dakki, M. & Ligny, W. de) 125–140 (Trav. Inst. Sci., 1988).

41. Dakki, M. & Ligny, W. de. *The Khnifiss lagoon and its sorrounding environment (Province of L'ayoune, Morocco)*. *Trav. Inst. Sci.* (1988).

42. Dakki, M. & Parker, D. M. The Khnifiss Lagoon and adjacent desert area: geographical description and recent coastline changes. in *The Khinifiss lagoon and its sorrouding environment (Province of L'ayoune, Morocco)* (eds. Dakki, M. & Ligny, W. de) 2–6 (1988).

43. Idrissi, J. L. *et al.* Organisation et fonctionnement d'un écosystème côtier du Maroc : la lagune de Khnifiss. *Revue des sciences de l'eau* **17**, 447–462 (2004).

44. Ait Brahim, Y. *et al.* Speleothem records decadal to multidecadal hydroclimate variations in southwestern Morocco during the last millennium. *Earth Planet Sci Lett* **476**, 1–10 (2017).

45. Nogueira, J. *et al.* Coastal wetland responses to a century of climate change in northern Sahara, Morocco. *Limnol Oceanogr* **67**, 285–299 (2022).

46. McGregor, H. V, Dima, M., Fischer, H. W. & Mulitza, S. Rapid 20th-Century Increase in Coastal Upwelling off Northwest Africa. *Science (1979)* **315**, 637–639 (2007).

47. Agbani, M. A. El, Fekhaoui, M., Bayed, A. & Schouten, J. R. The Khnifiss Lagoon and adjacent waters: hydrology and hydrodynamics. in *The Khnifiss Lagoon and its surrounding environment (Province of La'youne, Morocco)* (eds. Dakki, M. & Ligny, W. de) 17–26 (Trav. Inst. Sci., 1988).

48. Bond, G. *et al.* Persistent Solar Influence on North Atlantic Climate During the Holocene. *Science (1979)* **294**, 2130–2136 (2001).

49. Bond, G. *et al.* A pervasive millennial-scale cycle in North Atlantic Holocene and glacial climates. *Science (1979)* **278**, 1257–1266 (1997).

50. Cheddadi, R., Lamb, H. F., Guiot, J. & Van Der Kaars, S. Holocene climatic change in Morocco: A quantitative reconstruction from pollen data. *Clim Dyn* **14**, 883–890 (1998).

51. Mook, W. G. & van der Plicht, J. Reporting 14 C Activities and Concentrations. *Radiocarbon* **41**, 227–239 (1999).

52. Fægri, K. & Iversen, J. *Textbook of pollen analysis*. (John Wiley and Sons, 1989).

53. Roubik, D. W. & P., J. E. M. Pollen and Spores of Barro Colorado Island. *Kew Bull* **47**, 791 (1992).

54. Zonneveld, K. A. F. & Pospelova, V. A determination key for modern dinoflagellate cysts. *Palynology* **39**, 387–409 (2015).

55. Ndiaye, A. *et al.* Reconstruction of the holocene climate and environmental changes of Niayes peat bog in northern coast of Senegal (NW Africa) based on stable isotopes and charcoals analysis. *Quat Sci Rev* **289**, 107609 (2022).

56. Pannozzo, N., Smedley, R. K., Plater, A. J., Carnacina, I. & Leonardi, N. Novel luminescence diagnosis of storm deposition across intertidal environments. *Science of the Total Environment* **867**, 161461 (2023).

57. Peglar, S. M. *et al.* Terrestrial pollen record of recent land-use changes around nine North African lakes in the CASSARINA Project. *Aquat Ecol* **35**, 431–448 (2001).

58. Ballouche, A., Lefevre, D., Carruesco, C., Raynal, J. P. & Texier, J. P. Holocene environments of coastal and continental Morocco. *Quaternary Climate in Western Mediterranean* 517–531 (1986) doi:10.13140/2.1.1724.7529.

59. Winsemann, J., Hartmann, T., Lang, J., Fälber, R. & Lauer, T. Depositional architecture and aggradation rates of sand-rich, supercritical alluvial fans: Control by autogenic processes or high-frequency climatic oscillations? *Sediment Geol* **440**, (2022).

60. Torfstein, A., Gavrieli, I., Katz, A., Kolodny, Y. & Stein, M. Gypsum as a monitor of the paleo-limnological-hydrological conditions in Lake Lisan and the Dead Sea. *Geochim Cosmochim Acta* **72**, 2491–2509 (2008).

61. Parker, D., Bell, R. & Pye, S. Soils of the coastal platform between Khnifiss Lagoon and Tarfaya. in *The Khnifiss Lagoon and its surrounding environment (Province of La'youne, Morocco)* (eds. Mohamed Dakki & Ligny, W. De) 172 (Trav. Inst. Sci., 1988).

62. Martin-Puertas, C. *et al.* Regional atmospheric circulation shifts induced by a grand solar minimum. *Nat Geosci* **5**, 397–401 (2012).

63. Hurrell, J. W. Decadal Trends in the North Atlantic Oscillation: Regional Temperatures and Precipitation. *Science (1979)* **269**, 676–679 (1995).

64. Orme, L. C. *et al.* Aeolian sediment reconstructions from the Scottish Outer Hebrides: Late Holocene storminess and the role of the North Atlantic Oscillation. *Quat Sci Rev* **132**, 15–25 (2016).

65. Goslin, J. *et al.* Holocene centennial to millennial shifts in North-Atlantic storminess and ocean dynamics. *Sci Rep* **8**, 1–12 (2018).

66. Brayshaw, D. J., Hoskins, B. & Black, E. Some physical drivers of changes in the winter storm tracks over the North Atlantic and Mediterranean during the Holocene. *Philosophical Transactions of the Royal Society A: Mathematical, Physical and Engineering Sciences* **368**, 5185–5223 (2010).

67. Bakke, J., Lie, Ø., Dahl, S. O., Nesje, A. & Bjune, A. E. Strength and spatial patterns of the Holocene wintertime westerlies in the NE Atlantic region. *Glob Planet Change* **60**, 28–41 (2008).

68. Orme, L. C. *et al.* Past changes in the North Atlantic storm track driven by insolation and sea-ice forcing. *Geology* **45**, 335–338 (2017).

69. Bond, G. *et al.* A Pervasive Millennial-Scale Cycle in North Atlantic Holocene and Glacial Climates. *Science (1979)* **278**, 1257–1266 (1997).

70. Zielhofer, C. *et al.* Western Mediterranean hydro-climatic consequences of Holocene ice-rafted debris (Bond) events. *Climate of the Past* **15**, 463–475 (2019).

71. Deaton, C. D., Hein, C. J. & Kirwan, M. L. Barrier island migration dominates ecogeomorphic feedbacks and drives salt marsh loss along the Virginia Atlantic Coast, USA. *Geology* (2017) doi:10.1130/G38459.1.

72. Schuerch, M. *et al.* Future response of global coastal wetlands to sea-level rise. *Nature* (2018) doi:10.1038/s41586-018-0476-5.

73. Roman, C. T., Peck, J. A., Allen, J. R., King, J. W. & Appleby, P. G. Accretion of a New England (U.S.A.) salt marsh in response to inlet migration, storms, and sea-level rise. *Estuar Coast Shelf Sci* (1997) doi:10.1006/ecss.1997.0236.

74. Więski, K., Guo, H., Craft, C. B. & Pennings, S. C. Ecosystem Functions of Tidal Fresh, Brackish, and Salt Marshes on the Georgia Coast. *Estuaries and Coasts* **33**, 161–169 (2010).

75. FitzGerald, D. M. Shoreline Erosional-Depositional Processes Associated with Tidal Inlets. *Hydrodynamics and Sediment Dynamics of Tidal Inlets* **29**, 186–225 (1988).

76. Khalfaoui, O. *et al.* Paleoenvironmental evolution and evidence of marine submersion events from mid-to late Holocene in northwestern Morocco: The case of the Tahaddart lower estuary. *Cont Shelf Res* **256**, 104958 (2023).

77. Weisrock, A. L. E. Late-middle pleistocene, late pleistocene and holocene palaeo-sea-level records at agadir and the atlantic atlas coastal reach,morocco: An updated overview. *Quaternaire* **23**, 211–225 (2012).

78. Petit-Maire, N. Holocene biogeographical variation along the northwestern African coast (28 - 19 N). in *Sahara and the surrounding areas* (eds. Sarnthein, M., Seibold, E. & Rognon, P.) 365–377 (Balkema, 1980).

79. Zazo, C. *et al.* The coastal archives of the last 15ka in the Atlantic–Mediterranean Spanish linkage area: Sea level and climate changes. *Quaternary International* **181**, 72–87 (2008).

80. Lario, J. *et al.* Holocene palaeotsunami catalogue of SW Iberia. *Quaternary International* **242**, 196–200 (2011).

81. Ruiz, F. *et al.* Geomorphology Sedimentological and geomorphological imprints of Holocene tsunamis in southwestern Spain : An approach to establish the recurrence period. *Geomorphology* **203**, 97–104 (2013).

82. Jalut, G., Esteban Amat, A., Bonnet, L., Gauquelin, T. & Fontugne, M. Holocene climatic changes in the Western Mediterranean, from south-east France to south-east Spain. *Palaeogeogr Palaeoclimatol Palaeoecol* **160**, 255–290 (2000).

83. Santos, L., Sánchez-Goñi, M. F., Freitas, M. C. & Andrade, C. Climatic and environmental changes in the Santo André coastal area (SW Portugal) during the last 15,000 years. in *Quaternary climatic changes and environmental crises in the Mediterranean Region* 175–179 (2003).

84. Zielhofer, C., Bussmann, J., Ibouhouten, H. & Fenech, K. Flood frequencies reveal Holocene rapid climate changes (Lower Moulouya River, northeastern Morocco). *J Quat Sci* **25**, 700–714 (2010).

85. Olsen, J., Anderson, N. J. & Knudsen, M. F. Variability of the North Atlantic Oscillation over the past 5,200 years. *Nat Geosci* **5**, 808–812 (2012).

86. Holz, C., Stuut, J. B. W., Henrich, R. & Meggers, H. Variability in terrigenous sedimentation processes off northwest Africa and its relation to climate changes: Inferences from grain-size distributions of a Holocene marine sediment record. *Sediment Geol* **202**, 499–508 (2007).

87. Kim, J. H. *et al.* Impacts of the North Atlantic gyre circulation on Holocene climate off northwest Africa. *Geology* **35**, 387–390 (2007).

88. Bouimetarhan, I. *et al.* Palynological evidence for climatic and oceanic variability off NW Africa during the late Holocene. *Quat Res* **72**, 188–197 (2009).

89. Woodruff, J. D., Irish, J. L. & Camargo, S. J. Coastal flooding by tropical cyclones and sea-level rise. *Nature* **504**, 44–52 (2013).

90. Dezileau, L. *et al.* Intense storm activity during the Little Ice Age on the French Mediterranean coast. *Palaeogeogr Palaeoclimatol Palaeoecol* **299**, 289–297 (2011).

91. Cheddadi, R., Lamb, H. F., Guiot, J. & Van Der Kaars, S. Holocene climatic change in Morocco: A quantitative reconstruction from pollen data. *Clim Dyn* **14**, 883–890 (1998).

92. Knippertz, P., Christoph, M. & Speth, P. Long-term precipitation variability in Morocco and the link to the large-scale circulation in recent and future climates. *Meteorology and Atmospheric Physics* **83**, 67–88 (2003).

93. Jalali, B., Sicre, M.-A., Azuara, J., Pellichero, V. & Combourieu-Nebout, N. Influence of the North Atlantic subpolar gyre circulation on the 4.2 ka BP event. *Climate of the Past* **15**, 701–711 (2019).

94. McGee, D., deMenocal, P. B., Winckler, G., Stuut, J. B. W. & Bradtmiller, L. I. The magnitude, timing and abruptness of changes in North African dust deposition over the last 20,000 yr. *Earth Planet Sci Lett* **371–372**, 163–176 (2013).

95. Collins, J. A. *et al.* Rapid termination of the African Humid Period triggered by northern high-latitude cooling. *Nat Commun* **8**, 1372 (2017).

96. Roberts, N. *The Holocene: an environmental history*. (John Wiley & Sons, 2014).

97. Weisrock, A. *Geomorphologie et Paleoenvironments de l'Atlas atlantique, Maroc.* (Notes et Memoires du Service Geologique du Maroc, 1993).

98. Orme, L. C. *et al.* Past changes in the North Atlantic storm track driven by insolation and sea-ice forcing. *Geology* **45**, 335–338 (2017).

99. Weisrock, A. Geomorphologie et paleoenvironments de l'Atlas atlantique, Maroc. (Universite Paris I Pantheon-Sorbonne, 1980).

Acknowledgments

The authors acknowledge the French Research Institute for Development (IRD) for the facilities, personal, and financial support in the sample analysis, and field excursion. We also appreciate Ibn Zohr for hospitality and support during the development of this work. Elemental and isotopic analyses were performed at the ALYSES platform, at the Institute of Research for Development - IRD (Bondy, France). Thanks are also due to the Czech University of Life Sciences Prague for the financial support regarding the publication of this manuscript. The authors would like to thank the financial support provided by the CAPES (Coordination for the Improvement of Higher Education Personnel) and CNPq (Brazilian National Council for Scientific and Technological Development) through the primary author's scholarship and project development (CNPQ 457400/2012-9), respectively. L.B. acknowledges the support from CHARISMA Project with the assistance of the Hassan II Academy of Sciences, Morocco. J.N. would like to thanks Vinicios Gorito for the technical support.